Ice Basin Tests For Ice-Induced Vibrations Of Offshore Structures In The Shiver Project

Hendrikse, H.; Hammer, T.C.; Owen, C.C.; van den Berg, M.A.; van Beek, C.; Polojärvi, Arttu; Puolakka, Otto; Willems, Tom

DOI
10.1115/OMAE2022-78507

Publication date
2022

Document Version
Accepted author manuscript

Published in
Polar and Arctic Sciences and Technology

Proceedings of the ASME 2022 41st International Conference on Ocean, Offshore and Arctic Engineering
OMAE2022
June 5-10, 2022, Hamburg, Germany

OMAE2022-78507

ICE BASIN TESTS FOR ICE-INDUCED VIBRATIONS OF OFFSHORE STRUCTURES IN THE SHIVER PROJECT

Hayo Hendrikse
Delft University of Technology
Delft, Netherlands

Tim. C. Hammer
Delft University of Technology
Delft, Netherlands

Cody C. Owen
Delft University of Technology
Delft, Netherlands

Marnix van den Berg
Delft University of Technology
Delft, Netherlands

Kees van Beek
Delft University of Technology
Delft, Netherlands

Arttu Polojärvi
Aalto University
Espoo, Finland

Otto Puolakka
Aalto University
Espoo, Finland

Tom Willems
Siemens Gamesa Renewable Energy
The Hague, Netherlands

ABSTRACT

With the recent surge in development of offshore wind in the Baltic Sea, Bohai Sea and other ice-prone regions, a need has arisen for new basin tests to qualify the interaction between offshore wind turbines and sea ice. To this end, a series of model tests was performed at the Aalto ice basin as part of the SHIVER project. The tests were aimed at modeling the dynamic interaction between flexible, vertically-sided structures and ice failing in crushing. A real-time hybrid test setup was used which combines numerical and physical components to model the structure. This novel test setup enabled the testing of a wide range of structure types, including existing full-scale structures for which ice-induced vibrations have been documented, and a series of single-degree-of-freedom oscillators to obtain a better understanding of the fundamental processes during dynamic ice-structure interaction. The tests were primarily focused on the dynamic behavior of support structures for offshore wind turbines under ice crushing loads. First results of the campaign show that the combination of the use of cold model ice and not scaling time and deflection of the structure can yield representative ice-structure interaction in the basin. This is demonstrated with experiments during which a scaled model of the Norströmsgrund lighthouse and Molikpaq caisson were used. The offshore wind turbine tests resulted in multi-modal interaction which can be shown to be relevant for the design of the support structure. The dataset has been made publicly available for further analysis.

Keywords: Offshore wind, ice-structure interaction, scaling, frequency lock-in, intermittent crushing

1. INTRODUCTION

With the ongoing development of offshore wind in the Baltic Sea and Bohai Bay, ice-structure interaction has attracted significant attention the past years. For the preferred support structure concept of a tower on monopile foundation, the potential development of ice-induced vibrations needs to be considered in design.

The SHIVER project aims at addressing uncertainty with respect to these vibrations and is a collaboration between TU Delft, Siemens Gamesa Renewable Energy, and Aalto University. As part of the project, two basin test campaigns have been planned. The first one was executed in May and June, 2021, which is the focus in this paper. Data from that campaign are publicly available [1] and described in detail in [2]. The second campaign is planned for April 2023.

The first campaign was mainly aimed at gathering benchmark data for a state-of-the-art offshore wind turbine on monopile foundation interacting with drifting ice. Previous test campaigns targeting this same goal suffered from challenges related to scaling of the interaction, resulting in buckling failure of the ice rather than crushing [3], or focused only on the first global bending mode of the structure rather than the complete dynamics [4].

To overcome these challenges, it was attempted during the test campaign to alter the model ice at the Aalto Ice Tank to obtain a more stiff and brittle material behavior compared to traditional model ice. To allow for inclusion of the complete dynamics of offshore wind turbines, a real-time hybrid test setup was developed [5]. This setup combines numerical and physical

components to simulate a structure's response in ice. In such setup the focus is only on reproducing the motion of the structure at the ice action point in the physical domain, rather than that of the full structure. The full dynamic behavior is captured in the numerical domain where additional loads, such as wind loading on the structure, can be applied as well.

The main aims for the experimental campaign were defined as follows:

1. Develop a model-scale benchmark dataset for offshore wind turbines loaded by crushing ice.

2. Test the ice-structure interaction process for a series of single-degree-of-freedom (SDOF) oscillators to improve the fundamental understanding of ice-structure interaction processes.

3. Test models of existing full-scale structures for which ice-structure interaction is described in literature with the aim to validate the test approach and results.

4. Investigate the vibration frequency dependence of ice loads from model ice when interacting with a vertically sided cylinder which is forced to follow a sinusoidal vibration pattern in the horizontal plane (forced vibration testing).

5. Investigate the effect of ice speed on the mean, standard deviation and frequency content of ice loads from model ice failing in crushing against a rigid cylindrical pile.

In relation to aims 1, 2 and 5, the first analysis of the test results has already been completed. Part of the tests for offshore wind turbines in ice were aimed at validating numerical results used in the design of offshore wind support structures (aim 1) [6]. Experimental data showed that for the support structure of an offshore wind turbine in interaction with ice, the response is multi-modal and classical definitions of the interaction regimes (intermittent crushing, frequency lock-in, continuous brittle crushing) do not fully apply [7]. One example of multi-modal interaction observed in the experiments is shown in Figure 1. This type of interaction leads to the largest bending moments in the support structure of an offshore wind turbine when ice is concerned. The interaction and structural response are governed by the first global bending mode. When the structure moves towards the ice high amplitude oscillations of the second or third global bending mode are observed to develop.

The first analysis of the data gathered for SDOF structures (aim 2) has shown that the loads measured on a rigid pile as a function of indentation speed are representative for the loads on a flexible structure as a function of relative speed [8]. Further analysis of the onset of frequency lock-in during ice deceleration tests indicates that the damping from a positive gradient in the ice load dependence on indentation speed at high speeds seems to be key in predicting the onset velocity of lock-in. Additional experiments are required to confirm this positive trend for high speeds as the focus during the test campaign was mainly on indentation speeds below 0.15 m s^{-1}.

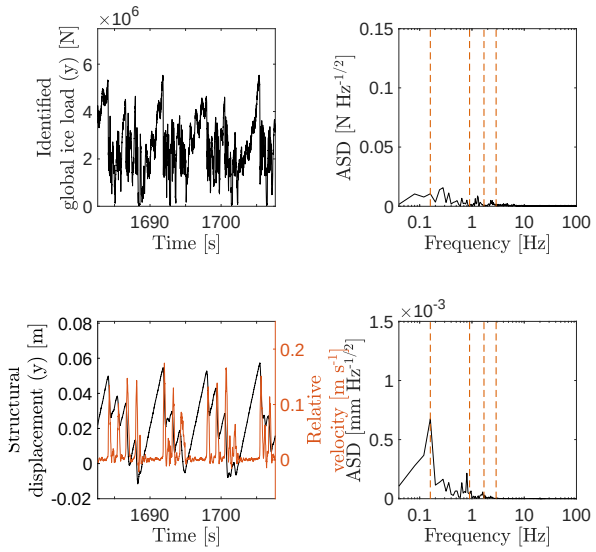

FIGURE 1: EXPERIMENTAL RESULT FOR AN IDLING OFFSHORE WIND TURBINE INTERACTING WITH SLOW MOVING ICE (TEST ID 593). TOP LEFT: TIME SERIES OF THE FULL-SCALE LOAD. TOP RIGHT: AMPLITUDE SPECTRAL DENSITY OF GLOBAL ICE LOAD. RED DASHED LINES INDICATE NATURAL FREQUENCIES OF THE STRUCTURE. BOTTOM LEFT: TIME SERIES OF STRUCTURAL RESPONSE. BOTTOM RIGHT: AMPLITUDE SPECTRUM OF STRUCTURAL RESPONSE [6].

The focus in this paper is on two particular aspects of the experimental campaign: 1) introduction of the colder model ice which was used during the experiments and observations on the differences between this type of model ice and the model ice traditionally used at the Aalto Ice Tank (Section 3), and 2) the results related to aim 3 for which a scaled version of the Norströmsgrund lighthouse and Molikpaq caisson were adopted in the experiments (Section 4). The analysis of the data of the forced vibration experiments (aim 4) and the effect of misalignment between wind and ice loading on the development of ice-induced vibrations (aim 1) are still ongoing at the time of writing.

2. EXPERIMENTAL CAMPAIGN

A detailed description of the test campaign and publicly available data are provided in [2]. In May and June of 2021, a total of 663 tests were conducted at the Aalto Ice Tank over a period of nine days in different types of ice. 259 tests have been qualified as successful, raw data and videos of which are publicly available [1]. Reasons for exclusion of data are related to physical limitations of the real-time hybrid test setup used, tests

performed in traditional model ice not being considered representative, and issues with carriage speed control early on in the campaign [2].

The test setup used was a real-time hybrid setup combining numerical and physical components allowing to simulate the response of different types of structures to ice loading with a single setup (Figure 2). Two linear actuators controlled the motion of the cylindrical test pile with 200 mm diameter. The ice load was measured on the pile using strain gauges and then fed to a controller which determined the response of the structure depending on the numerical model which could, for example, be a wind turbine, SDOF oscillator, or rigid pile. The response of the structure was then imposed on the pile by the linear actuators. This loop had an inherent delay of about 4.5 ms which was compensated for using a forward prediction algorithm [2].

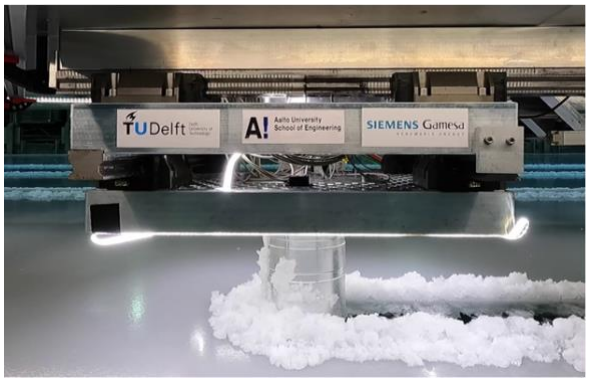

FIGURE 2: THE REAL-TIME HYBRID TEST SETUP DURING AN EXPERIMENT AT THE AALTO ICE TANK.

The setup was equipped with several measurement devices including accelerometers, load cells, strain gauges, magneto strictive displacement sensors and cameras. Raw data were measured and stored with 2000 Hz sampling frequency. During the experiments a carriage mounted under the bridge in the Aalto Ice Tank was used to move the setup through the ice with constant or varying speed. The carriage speed represented the ice drift speed in this way of testing.

In Section 4 of this paper, results are presented from test ID 448, 450, 453 and 454. These tests were all conducted on the 21st of June with an average ice thickness of 32 mm, a flexural strength of the ice of 500 kPa and compressive strength of 579 kPa. More information on the tests can be found in the database associated with the dataset [1].

3. COLD MODEL ICE AND TRADITIONAL MODEL ICE

One of the goals of the campaign was to try to make model ice which would not suffer from out-of-plane behavior not representative of crushing. In previous experiments by the authors with warm model ice, instability leading to bending failure had occurred often at lower speeds, preventing the development of intermittent crushing. Examples are given in [9] which are comparable to the observations by Barker et al. [3]. Furthermore, comments from the ice community on many past indentation experiments in model ice are that the ice looks to be too 'slushy' and 'ductile'. Though it is difficult to assess the impact of this visual difference on the validity of the tests, it is reasonable to state that the 'ductility' of the ice will have a significant influence on the development of ice-induced vibrations.

During the campaign a couple weeks were spent on altering the 'recipe' of growing the ice to obtain a material that is more brittle and stiffer than traditional model ice used in the Aalto Ice Tank. The best result in the time given was obtained by keeping the basin temperature at -11°C during the testing day (no tempering of the ice). This resulted in ice with a Young's modulus in the order of 10 GPa, average uniaxial compressive strength of 550 kPa and average bending strength of 450 kPa. These values were obtained using the standardized testing methods of the ITTC and are further elaborated upon in [2].

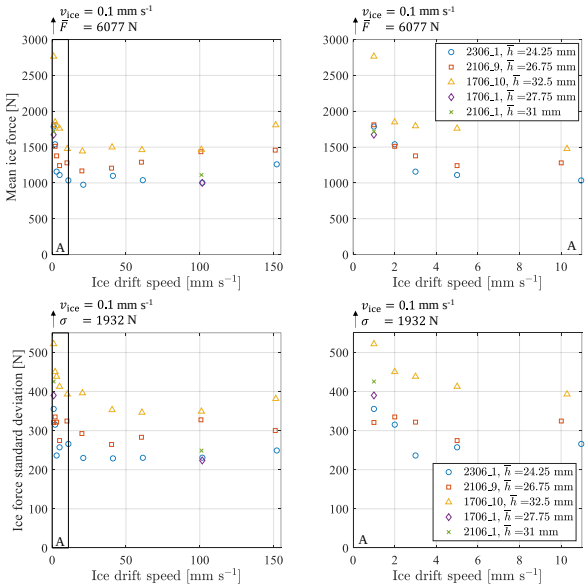

FIGURE 3: GLOBAL LOAD CHARACTERISTICS FOR THE COLD MODEL ICE. (TOP) MEAN LOAD AS A FUNCTION OF ICE DRIFT SPEED; (BOTTOM) STANDARD DEVIATION AS A FUNCTION OF ICE DRIFT SPEED (CARRIAGE SPEED IN THE EXPERIMENTS).

In addition to the standardized physical property tests a series of rigid indenter tests were conducted at the start of and throughout the day to obtain the load characteristics as a function of indentation speed for the ice. Examples of the trend in mean ice load and standard deviation of the load for such tests are shown in Figure 3. The focus was in particular on the range of 0.1 mm s^{-1} to 10 mm s^{-1}, as in this range the behavior of real ice was shown to change from simultaneous deformation of ice to non-simultaneous failure by Takeuchi et al. [10]. This change coincided with a corresponding reduction in global pressure by a factor of 2.5 – 6. For the cold model ice, a reduction in mean effective global pressure by a factor of 4.0 was obtained, when comparing a test at 0.1 mm s^{-1} and 100 mm s^{-1}. This matches the range of full-scale observations. The reduction in effective maximum pressure can be deduced from Figure 4 and amounts

to about a factor 6.25, though this is very much dependent on the duration of the test at high speed as longer runs inherently yield larger peaks and a lower factor between low and high-speed maximum loads.

Some example time series for the rigid indenter at different carriage speeds are shown in Figure 4 where it can clearly be seen that at the lowest indentation speed of 0.1 mm s^{-1} the behavior of the ice corresponds to a gradual increase in ice force and simultaneous deformation of the ice. Above 1 mm s^{-1} fluctuations with several peaks develop, corresponding to non-simultaneous failure. Takeuchi et al. [10] reported this change in behavior to occur for a ratio of ice speed over thickness v/h around 3 10^{-3}; in the experiments a similar value between 3 10^{-3} and 3 10^{-4} was found, which in part justifies not scaling the time-dependent processes during indentation when testing flexible structures as described further in Section 4.

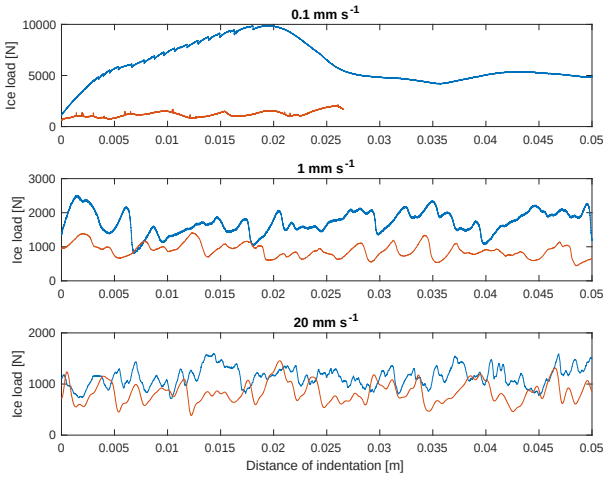

FIGURE 4: GLOBAL LOAD ON A RIGID STRUCTURE AS A FUNCTION OF INDENTATION DISTANCE FOR THREE DIFFERENT SPEEDS AS MEASURED DURING THE CAMPAIGN. THE COLD MODEL ICE IS SHOWN IN BLUE AND THE TRADITIONAL MODEL ICE IS SHOWN IN RED (TEST ID 85, 94, 120, 467, 474, 476).

During the campaign limited time was spent testing the traditional model ice as the aim was to overcome the challenges associated with it. One finding from the rigid structure tests is that the load reduction from low to high speed does not seem to be present in the traditional model ice, at least over the range of tested speeds (Figure 4). This could be because the transition is at a speed lower than 0.1 mm s^{-1} for the model ice, but we are inclined to believe that the traditional model ice more easily synchronizes across the indenter as the peaks at higher speed are much rounder and sharp changes associated with fracture are not visible in the load record. It is one of the aims for the second basin campaign in 2023 to investigate these differences in more detail.

During the data analysis phase, a very clear example of the importance of the model ice properties for the dynamic ice-structure interaction was found. Figure 5 shows the interaction between an offshore wind turbine model and a sheet of cold model ice as well as traditional model ice which is tempered to - 1.5°C. The indentation is at relatively high speed (100 mm s^{-1}) resulting in small oscillations around the equilibrium in the colder ice, whereas the warmer model ice yields high amplitude oscillations of the structure with a period close to the second natural period representative of frequency lock-in.

It is noted here that sustained frequency lock-in such as often observed in tests where only a single structural mode is dominant in the interaction with the ice is difficult to obtain when multiple modes of a structure are interacting at the same time, as is typical for an offshore wind turbine [6]. The amplitude of oscillation however does indicate that we deal with a case of lock-in as it matches the observations by Toyama et al. [11] in terms of the ratio between maximum structural response velocity and ice drift speed being 1.0-1.5. This would result in a displacement amplitude of 18 – 27 mm for an ice speed of 100 mm s^{-1} and a natural frequency of the second mode of 0.88 Hz, which matches the amplitude range observed in the bottom plot of Figure 5.

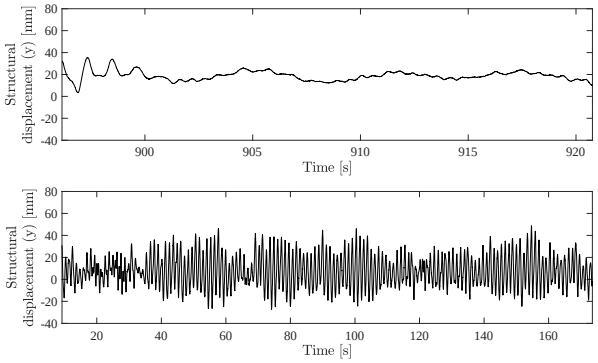

FIGURE 5: ICE-INDUCED VIBRATIONS DURING HIGH INDENTATION SPEED TESTS (HERE: 100 MM S^{-1}) OF AN OFFSHORE WIND TURBINE MODEL IN TWO MODEL ICE TYPES, TOP: -11°C COLD MODEL ICE; BOTTOM: -1.5°C TRADITIONAL MODEL ICE (TEST ID 603 AND 483).

The result shown in Figure 4 is quite striking and illustrates the challenge with scaling of model test results for ice-induced vibrations: Which of the two ice types yields the most representative full-scale result? Our preliminary results from testing structural configurations representative of the Norströmsgrund lighthouse and Molikpaq caisson indicate that the cold model ice might best capture the full-scale conditions (Section 4). A comparison to similar tests in traditional model ice is something which is still required to be done and would allow to say more about representativeness of results.

One last observation is that with the use of the cold model ice the ice keeps growing during the day, resulting in significant undergrowth at the end of a test day (Figure 6). The additional ice growth mostly consisted of slushy dendritic crystal growth with little apparent ice strength. However, the top of the additional growth layer would strengthen during the day, leading to a mild increase in measured ice loads on the structure and an increase in the measured ice thickness.

FIGURE 6: ICE VERTICAL CROSS SECTION AT THE END OF A TEST DAY (17-6-2021): A SPRAYED LAYER ON TOP, A LAYER OF INITIAL ICE THAT WAS FORMED BEFORE THE START OF THE SPRAYING PROCESS IN THE MIDDLE, AND A LAYER OF ADDITIONAL ICE GROWTH AT THE BOTTOM.

4. TESTS WITH MODELS OF EXISTING FULL-SCALE STRUCTURES

One of the main challenges in designing this test campaign was to deal with scaling for the experiments aimed at characterizing the offshore wind turbine in interaction with ice. There is no standard approach to scale dynamic ice-structure interaction, as the mechanisms relevant to dynamic ice-structure interaction are not yet fully understood. The ice normally used in model basins has been developed for bending failure of ice and has significant limitations when used to simulate interaction where ice fails in crushing. Scaling laws applied for ice bending, such as Froude or Cauchy scaling, do not govern the problem of crushing [12].

For this test campaign, the choice was made to not scale time, as the time-dependent behaviour of the ice in the basin could not be easily controlled and was not known in the planning phase of the experiments. Past experiments have shown that the ice drift speeds at which interactions develop in model ice tests (e.g. < 0.10 m s^{-1} [9]) are similar to full-scale observations (e.g. 0.023 to 0.075 m s^{-1} [13]). Based on this observation, and because of the absence of time scaling, the ice speed and the waterline displacements of the test structures were kept scale-invariant. Ziemer also proposed and discussed the merits of this type of scaling approach in a recent analysis [14].

To achieve structural deformations similar to full-scale, a mass scaling factor λ_m was applied to each mode of the structural models, affecting the mass (m), stiffness (k) and damping (c) of the structure. The scaling factor was determined based on the ratio between full-scale (FS) and model-scale (MS) mean brittle crushing load $\bar{F}$ at 100 mm s^{-1} indentation speed:

$$\boldsymbol{\lambda_m = \lambda_k = \lambda_c = \frac{\bar{F}_{FS}}{\bar{F}_{MS}}} \quad (1)$$

This approach ensures that the deformation of the structure in model-scale is equal to the full-scale deformation. For the Molikpaq cassion tests (ID 448 and ID449) a scale factor $\lambda_m = 75000$ and $\lambda_m = 25000$ were used, and for the Norströmsgrund lighthouse tests (ID 450, 453 and 454) a scale factor $\lambda_m = 2000$ was used.

It is noted that during the experiments the aspect ratio was fixed at about 6.7 which makes that it somewhat resembles a realistic situation for the Norströmsgrund lighthouse, though with relatively thick ice. For the Molikpaq, however, the aspect ratio is too small and the shape of the structure is also incorrect as only cylindrical indenters were used. The aspect ratio is assumed to matter in the transition between in-plane failure and out-of-plane failure after buckling instability and for the ratio between the variance and mean load during crushing. We assured that no buckling occurred during the tests by using ice with a high Young's modulus. The ratio between the ice load variance and mean load cannot be compared directly to full-scale. If a higher aspect ratio would have been used, the relative fluctuations of the load during continuous brittle crushing at high speed will be less than observed in the experiments. Furthermore, the aspect ratio may have an effect on the confinement of the ice in front of the indenter which is not accurately captured this way and would require further study to be quantified. For the effect of the structure shape on the interaction further tests are planned, though we expect the difference to mainly be a slight increase in load on a rectangle based on previous studies on this topic [15].

4.1 Results for the Molikpaq caisson

Test 448 and 449 were aimed at simulating an ice floe slowing down against a structure with dynamic properties defined as a scaled version of the Molikpaq platform. As a reference scenario the May 12th 1986 event was used [16]. During this event a large ice floe interacted with the structure resulting in the development of high-amplitude saw-tooth load and response patterns as the floe slowed down. This type of interaction is often referred to as 'intermittent crushing'. The change from stochastic brittle loading and associated structural response to repetitive saw-tooth loading with increasing period as the floe slows down is characteristic for this event. Another observation, also seen in the data from more slender structures in Cook Inlet [17] is that the peak global ice load increases when the saw-tooth loading pattern occurs.

As we did not have a full dynamic structural model of the Molikpaq available, an SDOF representation commonly used in numerical analysis was adopted [18]. The structural properties were a natural frequency of 1.3 Hz, damping ratio as a fraction of critical of 20 % and scaled mass-normalized modal amplitude of $2.24 \cdot 10^{-2}$ $kg^{-0.5}$. It is noted that this is an oversimplification of the platform which does not allow to capture any effect of higher modes on the interaction in the experiments and lumps too much stiffness to a single mode. The tests were started at an indentation speed of 0.06 m s^{-1} slowing down to 0 m s^{-1} over a time interval of 500 s.

Results for the global ice load are shown in Figure 7. The full-scale measurement data are also shown for reference and results for structural displacement are shown in Figure 8.

Qualitatively the interaction in the experiment developed similar to that observed in full-scale. For the higher ice drift speeds the ice load is stochastic with mean load fluctuations. As

the floe slows down the interaction results in the development of saw-tooth load and response patterns with increasing load amplitude for lower speeds as observed for the full-scale event. For the test where a lower scale factor was used (ID 449), only a few cycles of saw-tooth loading develop at the end of the signal when the structure is slowly indenting the ice. For the test with a higher scale factor (ID 448) the range of saw-tooth loading and load amplification is significantly larger.

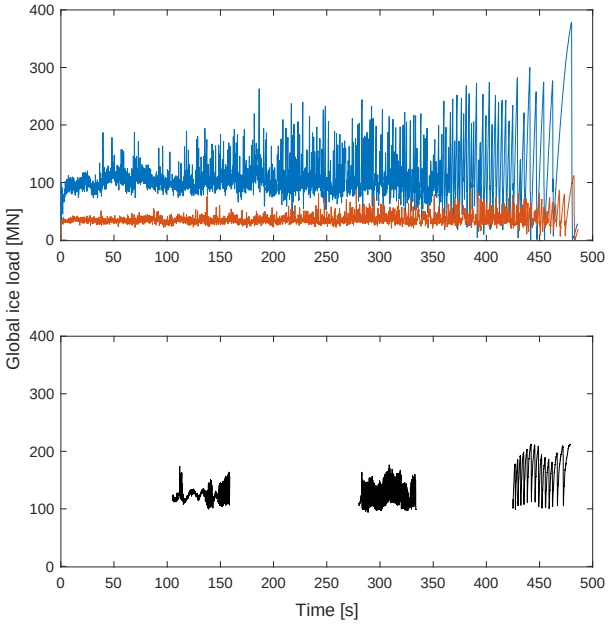

FIGURE 7: TEST CAMPAIGN LOAD DATA (TOP) AND FULL-SCALE MEASUREMENTS (BOTTOM) FROM THE MAY 12TH 1986 EVENT ON THE MOLIKPAQ. THE CAMPAIGN LOAD DATA HAVE BEEN FILTERED TO MATCH THE FILTERING OF THE LOAD PANELS USED IN FULL-SCALE. TEST ID 448 IS SHOWN IN BLUE AND TEST ID 449 IS SHOWN IN RED. THE FULL-SCALE BURST FILE DATA HAVE BEEN PLOTTED FOR RELATIVE COMPARISON AND THEREBY SHIFTED WITH RESPECT TO EACH OTHER AS THE EVENT DURATIONS DURING THE TEST AND IN REALITY WERE NOT SIMILAR.

Comparing the loads form the experiments to the full-scale observations it can be stated that the reality was somewhere in between the two tested scenarios. For test ID 448 the mean load at the start of the test seems to match well with the full-scale observation, but the loads at the end of the test are significantly higher than measured in full-scale. An explanation for this could be the background pressure from ice extrusion, crushed ice or rubble, which in the experiments is close to zero, but in full-scale may have contributed to the mean load. In a recent simulation study Gagnon applied a background load of 100 MN [19]. If that were to be added to the result from test ID 449 the load pattern matches relatively well with that observed in full-scale.

It is noted that an exact match in terms of loads is perhaps not the most interesting to pursue given that there also exists uncertainty with respect to the actual loads measured on the Molikpaq in 1986 [20].

Looking at the displacements in Figure 8 it can be seen that the mean displacement in the experiments is much lower than that measured. This can be explained by the single mode representation of the structure for which it is impossible to incorporate both a correct oscillating mass for the first eigenmode of the platform and a correct static waterline stiffness which consists of the contribution of all modes of the platform. In terms of amplitude of oscillation in the sawtooth part test ID 449 seems to be closest to reality.

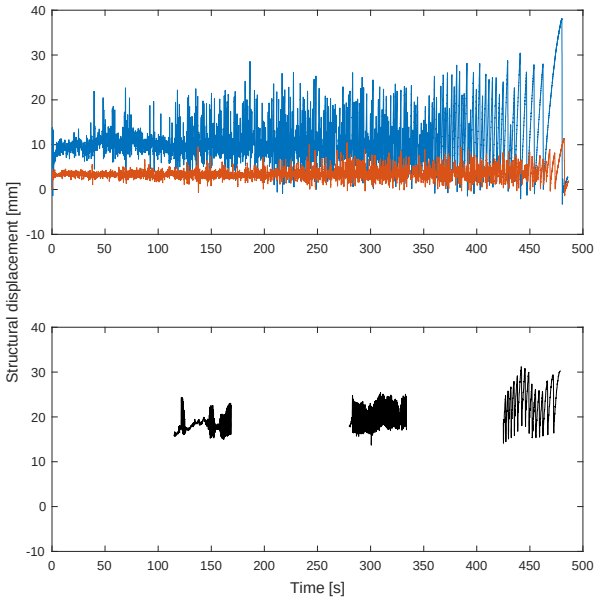

FIGURE 8: TEST CAMPAIGN DISPLACEMENT DATA AND FULL-SCALE MEASUREMENTS FROM THE MAY 12TH 1986 EVENT ON THE MOLIKPAQ. THE CAMPAIGN DISPLACEMENT DATA HAVE BEEN FILTERED TO MATCH THE FILTERING OF THE STRAIN GAUGES USED TO OBTAIN THE FULL-SCALE DATA. TEST ID 448 IS SHOWN IN BLUE AND TEST ID 449 IS SHOWN IN RED. THE FULL-SCALE BURST FILE DATA HAVE BEEN PLOTTED IN TIME FOR RELATIVE COMPARISON TO THE EXPERIMENT AS THE EVENT DURATIONS WERE NOT SIMILAR. THE LAST BURST FILE HAS BEEN CORRECTED FOR DRIFT [20].

4.2 Results for the Norströmsgrund lighthouse

The second full-scale structure tested during the experimental campaign is the Norströmsgrund lighthouse. Full-scale experience there has shown that the saw-tooth type loading and response associated with ‘intermittent crushing’ as observed for the Molikpaq did not develop, or perhaps only for a few cycles. Frequency lock-in has been observed to occur for short periods of time often in the order of 10 – 20 seconds, see Fig. 14 – Fig. 18 in [13]. These observations are often attributed to the lighthouse being relatively stiff for the ice conditions it is exposed to.

For this structure the aim was not to reproduce any particular event. Instead, we chose a relatively high full-scale load to verify that indeed under such high loading the saw-tooth patterns as we observed in the experiments for the Molikpaq would not develop and only short intervals of frequency lock-in would be encountered. The reference mean brittle crushing load for full-scale was about 2 MN, resulting in peak loads of 5-6 MN which are in line with the highest loads observed during the full-scale measurement campaigns [21].

The modal domain structural model used was taken from [22], including the first 16 global modes for the experiments. The tests were conducted as deceleration tests starting at an indentation speed of 0.1 m s^{-1} and ending at 0 m s^{-1} over a time interval of 260 s.

Results for the ice load and structural displacement are shown in Figure 9 and Figure 10. The load does not show the periodic saw-tooth displacement pattern developing, except during the last few seconds when the ice comes to a stop. A significant increase in the load for the lowest speeds is not observed as for the Molikpaq. A short period of frequency lock-in is observed around 140 s and around 200 s.

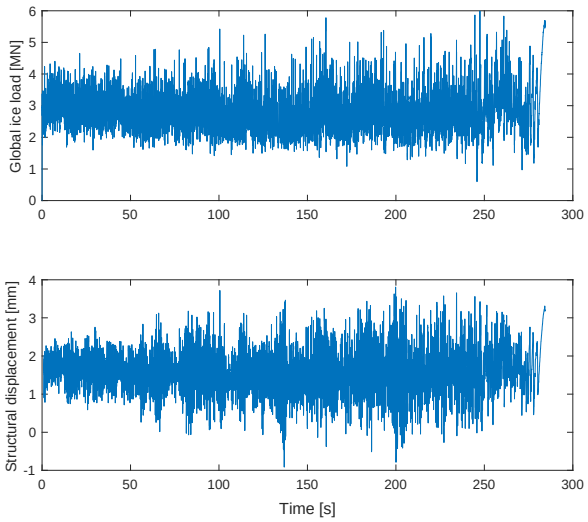

FIGURE 9: ICE LOAD AND STRUCTURAL DISPLACEMENT OF THE LIGHTHOUSE FOR A CONSTANT DECELERATION TEST. DATA ARE FILTERED WITH A 10 HZ BUTTERWORTH FILTER.

A zoom-in of the second event is given in Figure 10 showing the characteristic harmonic response pattern of the structure with a maximum displacement amplitude of about 1.7 mm. This corresponds to a velocity amplitude of the structure of about 26 mm s^{-1} which is about the ice speed as expected for frequency lock-in based on the relationship found by Toyama et al. [11]. It is noted again that for this particular structure frequency lock-in almost never lasted more than 10 – 20 seconds in the years during which full-scale measurements were conducted [13]. This is contrary to the statement which is often made that frequency lock-in is necessarily a long duration sustained type of interaction. The ice drift speeds of 0.05 m s^{-1} and 0.025 m s^{-1} for which frequency lock-in briefly developed during the tests correspond well to those reported for the full-scale events (0.02 m s^{-1} to 0.06 m s^{-1}).

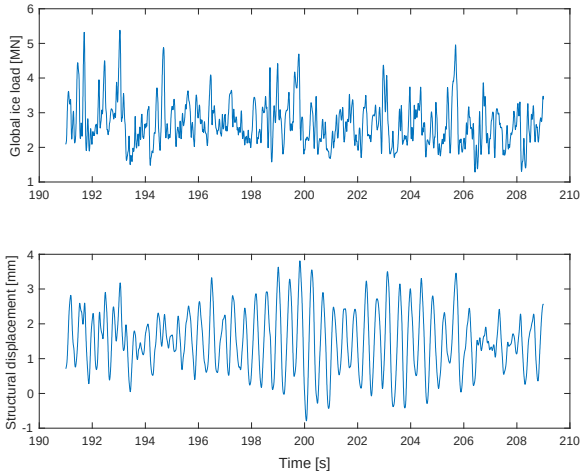

FIGURE 10: SHORT FREQUENCY LOCK-IN EVENT FOR THE NORSTRÖMSGRUND LIGHTHOUSE EXPERIMENT AROUND 200 S INTO THE TEST. THE ICE DRIFT SPEED AT THIS MOMENT WAS ABOUT 25 MM S^{-1}. DATA ARE FILTERED WITH A 10 HZ BUTTERWORTH FILTER. SEE FIGURE 14-18 IN [13] FOR COMPARABLE SHORT DURATION EVENTS FROM THE FULL-SCALE MEASUREMENTS AT THE NORSTRÖMSGRUND LIGHTHOUSE.

4.3 Discussion

We find that the chosen scaling approach has merit given the development of saw-tooth displacement and load patterns for the Molikpaq test, and given the absence of such interaction for the Norströmsgrund lighthouse. The erratic development of frequency lock-in for the Norströmsgrund lighthouse test reflects full-scale observations well. Response amplitudes for both structures are in range of those reported in full-scale, giving confidence in the scalability of the test campaign results.

A question which requires further attention is the scalability of the ‘static’ pressure due to the presence of crushed ice or rubble at the ice-structure interface. This pressure is likely to be related to the displaced volume of each which in our tests does not scale the same way as the load from the intact ice. If there is indeed such static background pressure it can be easily added after the experiments as it would result only in a mean offset of the displacement of the structure. Determining the fraction of the full-scale measured loads associated with crushed ice or rubble is unfortunately not straightforward.

Effect of shape and aspect ratio remain to be investigated. It is expected that our use of a smaller aspect ratio results in more variance of the brittle crushing load for example. For the more structure-dominated interaction at low speed, the effect of the

incorrect scaling of aspect ratio is then expected to be minor. These aspects are to be further investigated in the second test campaign in 2023.

5. CONCLUSION

Basin tests for dynamic ice-structure interaction were performed using for the first time a real-time hybrid test setup in an ice tank. By controlling the temperature, cold crushing model ice could be developed which showed characteristics comparable to real ice. These characteristics are the change from simultaneous deformation to non-simultaneous failure at a loading rate v/h of about 10^{-3} s^{-1} in conjunction with a reduction in maximum effective pressure by a factor three to six, as well as a Young's modulus in the order of 10 GPa.

A scaling method was adopted which has been demonstrated to give representative results for dynamic ice-structure interaction in an ice basin when compared with full-scale data from the Norströmsgrund lighthouse and Molikpaq caisson. Interaction with scaled offshore wind turbine models showed new regimes of ice-induced vibrations particular for these structures which are relevant for design of the support structure.

Data from forced vibration experiments, the influence of wind and wind-ice misalignment on dynamic ice-structure interaction are still being analyzed. A follow-up test campaign is planned for April 2023. For that campaign the focus will be on closing data gaps such as: testing with different shape indenters, more extensive testing with different ice types, and having a full offshore wind turbine represented in the numerical part of the setup including the non-linear interaction with the wind.

ACKNOWLEDGEMENTS

The authors thank the participating organizations in the SHIVER project: TU Delft, Siemens Gamesa Renewable Energy, and Aalto University, for supporting this work.

We further thank Jeroen Koning and the colleagues from DEMO at TU Delft for the design and manufacturing of the mechanical parts of the test setup. We thank the crew of the Aalto Ice Tank: Teemu Päivärinta, Lasse Turja and Sampo Hanhirova, for their help in preparation and installation of the setup and dedication to the execution of the tests.

Funding: This work was supported by TKI-Energy by the 'Toeslag voor Topconsortia voor Kennis en Innovatie (TKI's)' of the Dutch Ministry of Economic Affairs and Climate Policy. (grant reference: TKITOE_WOZ_1906_TUD_SHIVER).

REFERENCES

[1] Hendrikse, H., Hammer, T., van den Berg, M., Willems , T., Owen, C.C., van Beek, K., Ebben, N., Puolakka, O., Polojärvi, A., 2021, "Data from ice tank tests with vertically sided structures collected during the SHIVER project," 4TUResearchData Dataset, https://doi.org/https://doi.org/10.4121/17087462.v1

[2] Hendrikse, H., Hammer, T.C., van den Berg, M., Willems, T., Owen, C.C., van Beek, K., Ebben, N.J.J., Puolakka, O., Polojärvi, A., 2022, "Experimental data from ice basin tests with vertically sided cylindrical structures," *Data in Brief,* 41, 107877. https://doi.org/10.1016/j.dib.2022.107877

[3] Barker, A., Timco, G.W., Gravesen, H., Vølund, P., 2005, "Ice loading on Danish wind turbines. Part 1: Dynamic model tests," *Cold Reg. Sci. Technol.*, 41(1), pp. 1–23. https://doi.org/10.1016/j.coldregions.2004.05.002

[4] Tian, Y., Huang, Y., Li, W., 2019, "Experimental Investigations on Ice Induced Vibrations of a Monopile-type Offshore Wind Turbine in Bohai Sea," ISOPE-I-19-285, Paper presented at the The 29th International Ocean and Polar Engineering Conference, Honolulu, Hawaii, USA, June 2019.

[5] Hammer, T.C., van Beek, K., Koning, J., Hendrikse, H., 2021, "A 2D test setup for scaled real-time hybrid tests of dynamic ice- structure interaction.", Proc. 26th Int. Conf. Port Ocean Eng. under Arct. Cond., Moscow, Russian Federation, POAC21-024.

[6] Hammer, T.C., Willems, T., Hendrikse, H., 2022, "Dynamic ice loads for offshore wind turbine support structure design," *Mar. Struct.* (submitted).

[7] Hammer, T.C., Owen, C.C., van den Berg, M., Hendrikse, H., 2022, "Classification of ice-induced vibration regimes of offshore wind turbines," Proceedings of the ASME 2022 41st International Conference on Ocean, Offshore and Arctic Engineering, OMAE2022, June 5-10, 2022, Hamburg, Germany.

[8] Van den Berg, M.A., Owen, C.C., Hendrikse, H., 2022, "Experimental study on ice-structure interaction phenomena of vertically sided structures," *Cold Reg. Sci. Technol.* (submitted).

[9] Hendrikse, H., Ziemer, G., Owen, C.C., 2018, "Experimental validation of a model for prediction of dynamic ice-structure interaction," *Cold Reg. Sci. Technol.*, 151, pp. 345–358. https://doi.org/10.1016/j.coldregions.2018.04.003

[10] Takeuchi, T., Sakai, M., Akagawa, S., Nakazawa, N., Saeki, H., 2001, "On the factors influencing the scaling of ice forces," in: IUTAM Symp. Scaling Laws Ice Mech. Ice Dyn., Springer, 2001: pp. 149–160.

[11] Toyama, Y., Sensu, Y., Minami, M., Yashima, N., 1983, "Model tests on ice-induced self-excited vibration of cylindrical structures," Proceedings, 7th International Conference on Port and Ocean Engineering Under Arctic Conditions. vol. II, pp. 834–844.

[12] Palmer, A.C., Dempsey, J.P., 2009, "Model tests in ice," in: Proceedings, Twent. Int. Conf. Port Ocean Eng. under Arct. Cond., Luleå, Sweden.

[13] Nord, T.S., Samardžija, I., Hendrikse, H., Bjerkås, M., Høyland, K.V., Li, H., 2018, "Ice-induced vibrations of the Norströmsgrund lighthouse," *Cold Reg. Sci. Technol.*, 155, pp. 237–251.

https://doi.org/10.1016/j.coldregions.2018.08.005
[14] Ziemer, G., 2021, *Ice-Induced Vibrations of Vertical Structures*, Doctoral thesis, Technischen Universität Hamburg.
[15] Owen, C.C., Hendrikse, H., 2018, "Ice-Induced Vibrations of Model Structures with Various Dynamic Properties," Proc. 24th IAHR International Symposium on Ice, Vladivostok, Russia, pp. 376 – 385.
[16] Gagnon, R.E., 2012, "An explanation for the Molikpaq May 12, 1986 event," *Cold Reg Sci Technol*., 82, pp. 75–93. https://doi.org/10.1016/j.coldregions.2012.05.009
[17] Blenkarn, K.A., 1970, "Measurement and analysis of ice forces on cook inlet structures," Paper presented at the Offshore Technology Conference, Houston, Texas, April. https://doi.org/10.4043/1261-MS
[18] Kärnä, T., Andersen, H., Gürtner, A., Metrikine, A., Sodhi, D., Loo, M., Kuiper, G., et al., 2013, "Ice-Induced Vibrations of Offshore Structures – Looking Beyond ISO 19906," in: Proc. 22nd Int. Conf. Port Ocean Eng. under Arct. Cond., Espoo, Finland, pp. 1–12.
[19] Gagnon, R., 2022, "Spallation-based numerical simulations of ice-induced vibration of structures," *Cold Reg. Sci. Technol.*, 194, 103465. https://doi.org/10.1016/j.coldregions.2021.103465
[20] Owen, C.C,, Hendrikse, H., 2021, "Simulation and analysis of ice-induced vibrations experienced by Molikpaq during the May 12 , 1986 event," Proc. 26th Int. Conf. Port Ocean Eng. under Arct. Cond., Moscow, Russian Federation, POAC21-062.
[21] Frederking, R., 2005, "Tiltmeter application at norströmsgrund lighthouse - Strice project," Proc. 18th Int. Conf. Port Ocean Eng. under Arct. Cond. POAC, vol. 1, Potsdam, New York, USA: 2005, pp. 399–408.
[22] Hendrikse, H., Nord, T.S., 2019, "Dynamic response of an offshore structure interacting with an ice floe failing in crushing," *Mar. Struct.*, 65, pp. 271–290. https://doi.org/10.1016/j.marstruc.2019.01.012